

Investigating the effects of ocean layering and sea ice cover on acoustic propagation in the Beaufort Sea

Jason D. Sagers, Megan S. Ballard, and Mohsen Badiey

Citation: [Proc. Mtgs. Acoust.](#) **25**, 005003 (2015); doi: 10.1121/2.0000316

View online: <https://doi.org/10.1121/2.0000316>

View Table of Contents: <https://asa.scitation.org/toc/pma/25/1>

Published by the [Acoustical Society of America](#)

ARTICLES YOU MAY BE INTERESTED IN

[Measured and modeled acoustic propagation underneath the rough Arctic sea-ice](#)

The Journal of the Acoustical Society of America **142**, 1619 (2017); <https://doi.org/10.1121/1.5003786>

[Acoustic signal and noise changes in the Beaufort Sea Pacific Water duct under anticipated future acidification of Arctic Ocean waters](#)

The Journal of the Acoustical Society of America **142**, 1926 (2017); <https://doi.org/10.1121/1.5006184>

[Properties of the ambient noise field at the 150-m isobath during the Canada Basin Acoustic Propagation Experiment](#)

Proceedings of Meetings on Acoustics **33**, 070001 (2018); <https://doi.org/10.1121/2.0000839>

[Modeling acoustic wave propagation and reverberation in an ice covered environment using finite element analysis](#)

Proceedings of Meetings on Acoustics **33**, 070002 (2018); <https://doi.org/10.1121/2.0000842>

[The influence of the physical properties of ice on reflectivity](#)

The Journal of the Acoustical Society of America **77**, 499 (1985); <https://doi.org/10.1121/1.391869>

[Elastic parabolic equation and normal mode solutions for seismo-acoustic propagation in underwater environments with ice covers](#)

The Journal of the Acoustical Society of America **139**, 2672 (2016); <https://doi.org/10.1121/1.4946991>



POMA Proceedings
of Meetings
on Acoustics

**Turn Your ASA Presentations
and Posters into Published Papers!**





170th Meeting of the Acoustical Society of America

Jacksonville, FL
2-6 November 2015

Acoustical Oceanography: Paper 1pAO4

Investigating the effects of ocean layering and sea ice cover on acoustic propagation in the Beaufort Sea

Jason D. Sagers and Megan S. Ballard

Applied Research Laboratories, The University of Texas at Austin, Austin, TX; sagers@arlut.utexas.edu; meganb@arlut.utexas.edu

Mohsen Badiey

College of Earth, Ocean, & Environment, University of Delaware, Newark, DE; badiey@udel.edu

Over the past several decades, the Beaufort Gyre has experienced changes in sea-ice freshwater accumulation and ocean stratification which has implications for long-range acoustic propagation. In this talk, acoustic propagation from the Canadian Basin to the Alaskan Beaufort Shelf is modeled using measurements of physical oceanography and sea ice. Water masses that impact acoustic propagation and stratification in the basin include the warm, saline Atlantic Water (AW), which is overlain by cooler, less-saline Pacific Winter Water (PWW). Oceanographic observations reveal intrusions of a warmer, fresher water mass called Pacific Summer Water (PSW). This water mass resides below the surface mixed layer, but above the PWW and reduces acoustic interaction with the sea-ice canopy for source depths located in the halocline duct. Oceanographic data indicate that on the continental shelf, the PSW intrusion can be absent in the ice-covered months resulting in an upward refracting sound speed profile. Using measurements from ice-tethered profilers in the basin and oceanographic moorings on the shelf, we model the temporal and spatial variability of the acoustic field. The effect of scattering from the ice cover is included, with consideration given to the seasonal variability of sea-ice concentration, thickness, and acoustic properties.



1. Overview

This paper investigates environmental parameters affecting acoustic propagation between an acoustic source located in the Canadian Basin and a receiver located on the Chukchi continental shelf.¹ Such a propagation path will likely exist for much of the upcoming 2016-2017 CANadian basin Acoustic Propagation Experiment (CANAPE). A second objective of this paper is to approximately bound the range of transmission loss (TL) due to variability in some of the environmental parameters. The analysis is restricted in scope inasmuch as only ice-covered months are considered.

In this paper we provide a heuristic approach in assessing the changes that variable oceanographic modeling can have on acoustic wave propagation in this environment. The approach is to assemble environmental data measured previously, construct a set of range-dependent water column sound speed profile (WCSSP) realizations, compute acoustic fields for each realization, and then to investigate summary statistics describing the TL.

2. Environmental description

The nominal acoustic source and receiver locations are denoted as triangles on the map shown in Fig. 1. The major environmental parameters affecting acoustic propagation between these locations include the oceanography and the sea ice. Pacific water enters the Arctic Ocean though

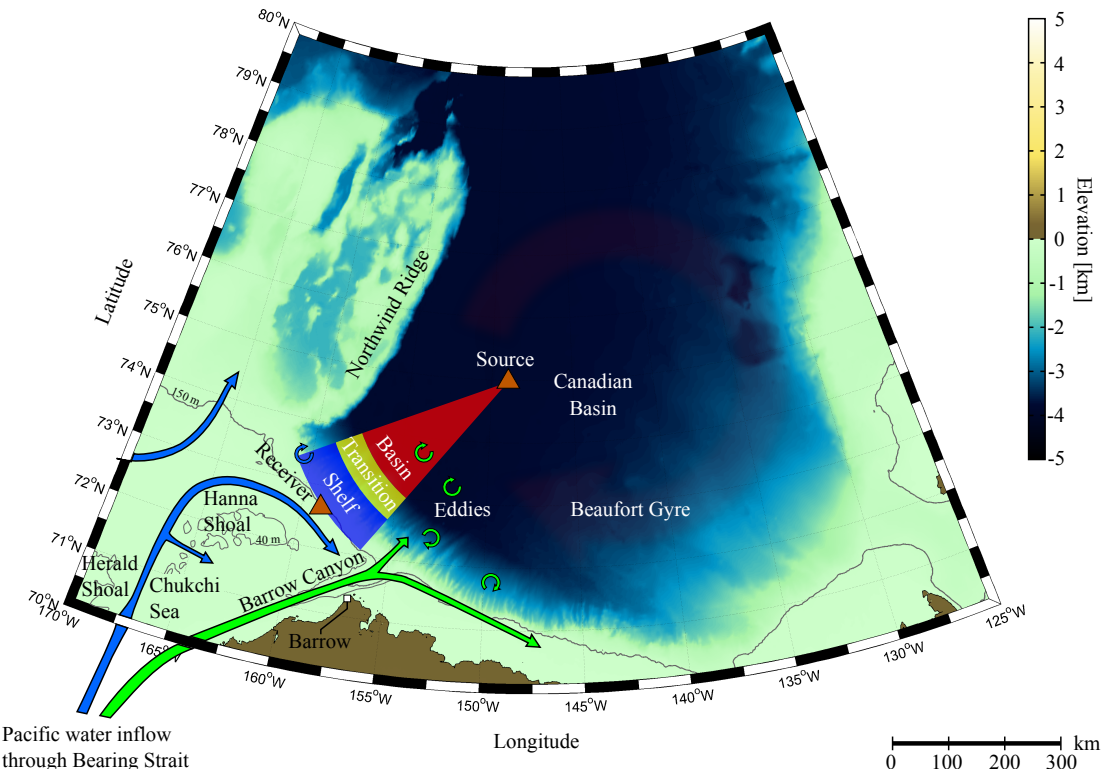


FIGURE 1: Map of the Chukchi Sea and Canadian Basin, with inflows marked after Ref. 2.

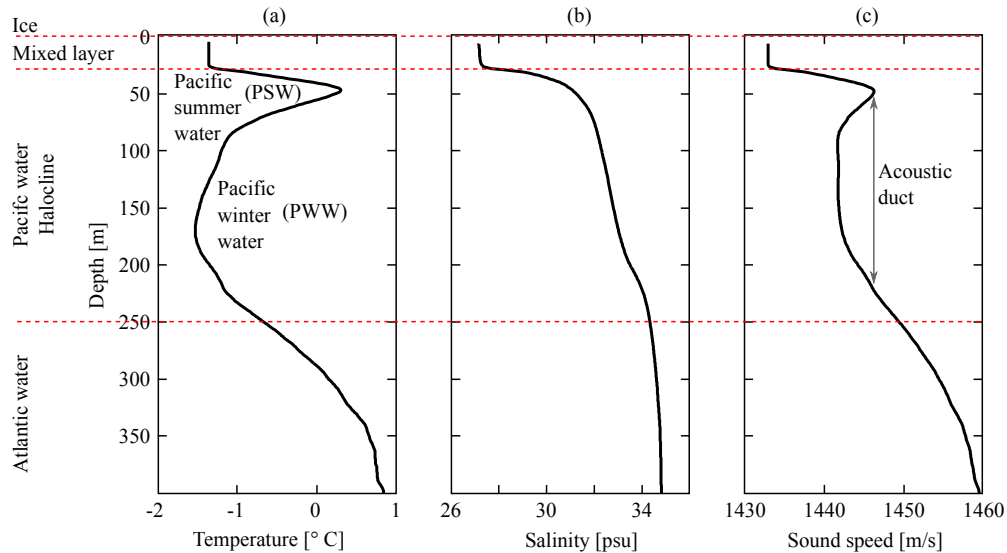


FIGURE 2: Typical vertical profile of (a) temperature, (b) salinity, and (c) sound speed as measured in the Canadian Basin by an ice-tethered profiler.

the Bering Strait, whereupon it spreads throughout the Chukchi Shelf and the northwest coast of Alaska. During winter months the Pacific-origin water is cooled on the shallow Chukchi shelf, while during summer months it is warmed by solar irradiation and river runoff. The Pacific-origin water is eventually transported into the Canadian Basin where it becomes the principal component of the halocline. The transport mechanisms of the Pacific-origin water into the Canadian Basin are believed to include eddy formation and propagation, and possibly direct outflow of water through Barrow Canyon.^{2–5} The Beaufort Gyre then controls the mesoscale circulation of the water mass in the Canadian Basin.

A typical vertical profile of temperature and salinity in the Canadian Basin as measured by an ice-tethered profiler (ITP) deployed by Woods Hole Oceanographic Institute (WHOI)⁶ is shown in Fig. 2(a) and (b), respectively. The Pacific-origin water constitutes the majority of the halocline, which extends between approximately 30 m and 250 m depth. The Pacific summer water (PSW) is warmer and less saline and consequently overlies the cooler Pacific winter water (PWW). Above the Pacific water mass and below the ice canopy is a surface mixed layer of near constant temperature and salinity. Below the Pacific water mass is warm, saline water originating from the Atlantic ocean.

Figure 2(c) shows the WCSSP computed from the temperature and salinity profiles of Fig. 2(a)-(b), and it is apparent that the ocean layering can create a double-ducted acoustic waveguide. The first duct lies between the ice canopy and the PSW layer. Sound trapped in this duct will undergo repeated interactions with the ice and will be subject to relatively high transmission loss. The second duct lies between the PSW layer and the Atlantic water layer. Sound paths launched horizontally from a source located in this duct might be shielded from interaction with the ice, experience lower transmission loss, and propagate longer distances. The degree to which the duct can channel acoustic energy depends largely on the properties of the PSW and PWW layers. For the remainder of this paper, the acoustic duct of interest is the lower duct which has the potential to propagate sound to longer ranges.

Spatial and temporal variability of the typical profile does exist. One source of localized

variability arises from eddies which form along the Chukchi and Beaufort shelves and then propagate into the basin^{5,7–10} (depicted schematically in Fig. 1). The eddies are predominantly cold-core and many exist near the top of the halocline layer. From an acoustic propagation standpoint, a cold-core eddy in the PSW layer could locally decrease the sound speed gradient near the top of the duct, resulting in additional sound escaping from the duct. The range variability of the Pacific water layer is one of the environmental factors investigated from an acoustic point of view in this paper.

The typical vertical profile shown in Fig. 2 is prevalent throughout the Central and Western Canadian Basin.¹¹ The portion of the acoustic propagation track where the authors deemed it a reasonable approximation to apply basin WCSSPs is indicated by the red wedge in Fig. 1. An upward-refracting WCSSP has been observed on the continental shelf during ice-covered months. Therefore for some range extending from the receiver out toward the source (indicated by the blue wedge in Fig. 1), the sound will not be trapped in an acoustic duct and will be free to refract upward and interact with the ice canopy. Over these ranges, the properties of the sea ice will likely have the largest impact on the transmission loss. For this reason, the assumed ice properties is another environmental factor considered in this paper.

It is surmised that there is a transition region between the shelf and basin where the acoustic duct would terminate and the upward-refracting WCSSP would become critical to the acoustic propagation. Unfortunately, the authors have been unable to find oceanographic measurements in this location during ice-covered months that could better constrain this portion of the propagation track. This is an important disclaimer for the accuracy of the oceanographic model employed in this paper.

3. Environmental measurements

Basin oceanographic measurements

A multitude of environmental measurements have been made in the Arctic in recent decades and the authors are fortunate to utilize several such measurements. Specifically, the authors recognize the ITP project,⁶ the Shelf-Basin Interaction (SBI) project,¹² and the Beaufort Gyre Exploration Project (BGEP)¹³ as having produced data particularly useful for this analysis. Some of the oceanography measurements made by these programs will be used to construct a set of WCSSPs which will then become inputs to an acoustic propagation model.

Six ITP data sets,⁶ whose drift tracks are shown in Fig. 3, were selected for use in this work based on the relative proximity of their drift track to the acoustic propagation path and their relatively recent measurement dates. The ITP drifts with the ice sheet over the course of its deployment, making measurements at preprogrammed intervals. Consequently, there is an inherent spatio-temporal ambiguity in sampling the water column which cannot be resolved from the data themselves. Using the reported GPS time and position reported for each profile, the data can be displayed as a function of cumulative distance along the drift track.

The data for ITP 34 and ITP 86 are shown in Fig. 4. Of the six ITP data sets, ITP 18, 34, and 35 measured a slightly *cooler* PSW layer (with maximum temperatures between -0.5 to 0° C) than the *warmer* ITP 69, 78, and 86 (which had maximum PSW temperatures between 0 to 0.5° C). An example of this difference is seen by looking for the maximum temperature of the PSW layer (near 50-60 m depth) in the first column of Fig. 4. The temperature of the PSW layer will be investigated in this paper by examining the differences between the two groups (*warmer* and *cooler*) of ITP

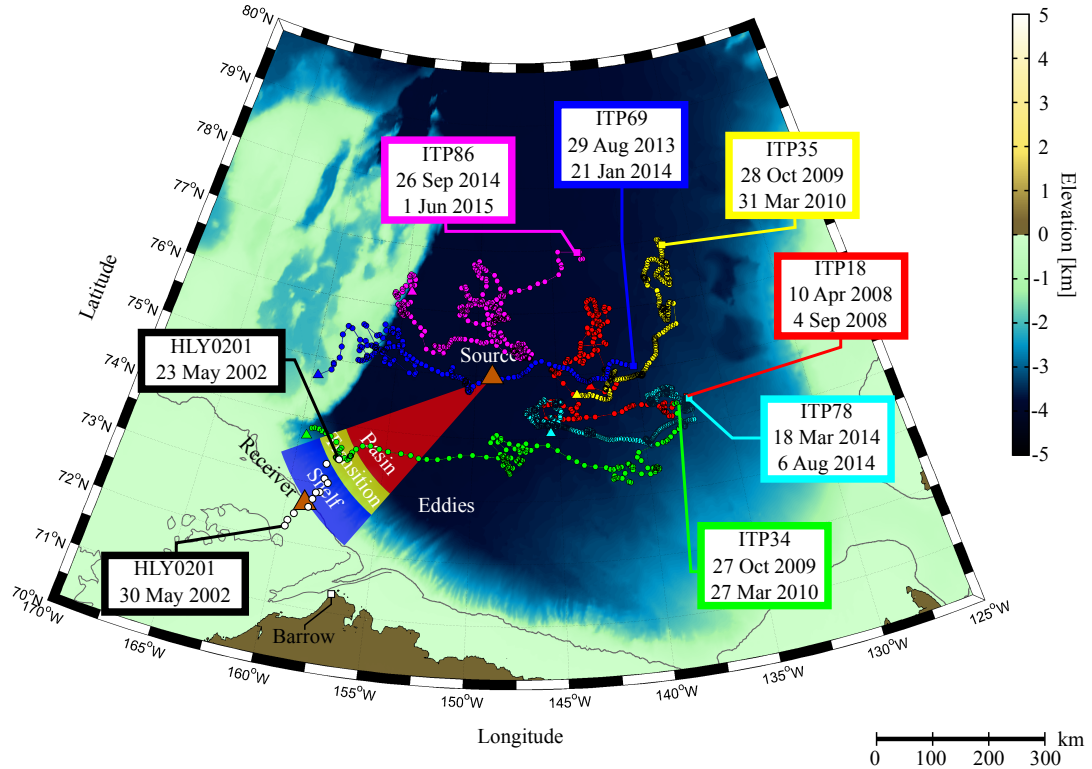


FIGURE 3: Locations of oceanographic measurement locations consisting of six ITP drift tracks and 11 Healy CTD stations.

measurements. This difference might be significant as the sound speed gradient near the top of the acoustic duct, seen by comparing the third column of Fig. 4, is clearly influenced by temperature.

Shelf/slope oceanographic measurements

A cruise of the United States Coast Guard Healy during May 2002 made multiple conductivity, temperature, and depth (CTD) measurements on the Chukchi Shelf and over the continental slope (see Fig. 3 for the station locations). This hydrographic transect is particularly useful because there was still ice cover over the area, it contains the upward refracting WCSSP on the shelf, and the transect extends far enough into the basin to identify the edge of the PSW layer. This measurement gives one observation of where the transition region might end and the more stable basin profiles might begin during ice covered months.

Ice draft measurements

Direct measurements of ice draft near the North Pole were made by an undersea vehicle with an upward looking sonar in July 2005.¹⁴ These data are used to compute the surface reflection coefficient in the acoustic propagation model. The ice at the North Pole is expected to be rougher than the ice covering the acoustic propagation path. Nevertheless, these data were applied to give the worst case scattering loss from the ice canopy.

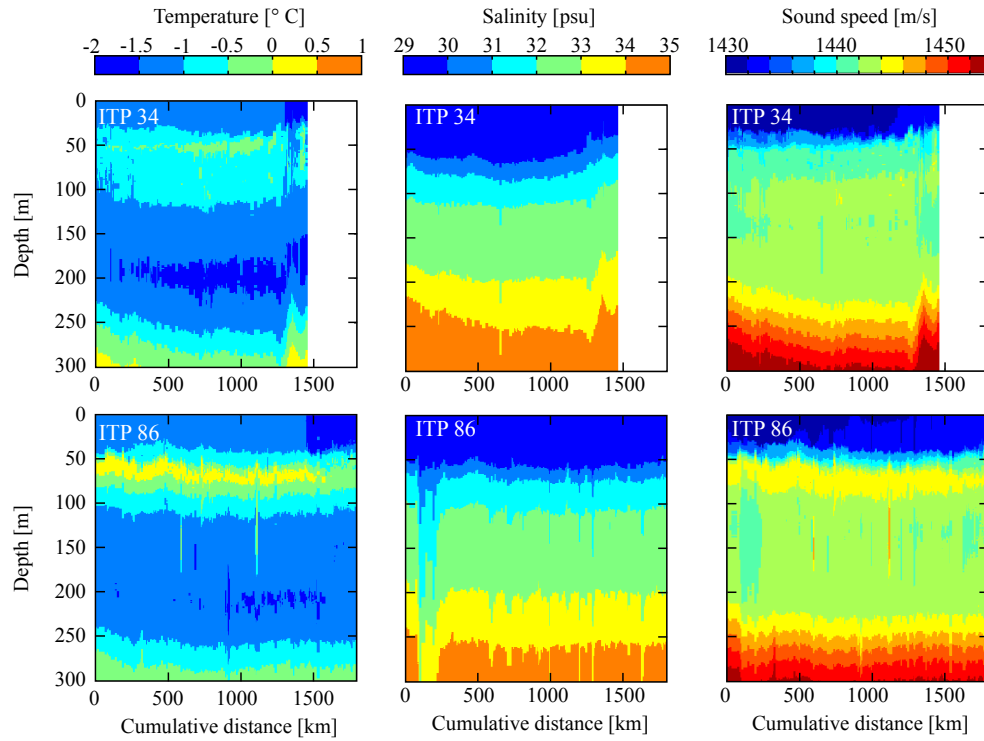


FIGURE 4: Vertical profiles of temperature and salinity data from ITP 34 (top row) and ITP 86 (bottom row). The third column is the computed sound speed. The data are shown as a function of cumulative distance along the drift track.

4. Data assimilation and acoustic model

This section discusses how the environmental measurements were applied to create WCSSP realizations and additional details of the acoustic propagation model. The acoustic propagation path spans 400 km from the center of the Canadian Basin to the 150 m isobath on the Chukchi Shelf. The bathymetry along this path was extracted from the International Bathymetric Chart of the Arctic Ocean (IBCAO) Version 3.0.¹⁵

Both range-dependent and range-independent WCSSP realizations were created numerically as inputs for an acoustic propagation model. To construct a range-dependent WCSSP, the section of the water column along the acoustic propagation path from 0 to 250 km is populated by a subset of the measured ITP data. Different realizations are made by populating the first 250 km of the track with different 250 km subsets of ITP data (each ITP measurement contained about 1500 km of cumulative drift distance, allowing for about six potential realizations per ITP data set). The section of the water column from 310 to 400 km is populated by the Healy 2002 hydrographic transect data, which was interpolated in range between the measurement locations, and remains constant between realizations. The section of the water column from 250 to 310 km is linearly interpolated between the ITP data and the Healy transect data and therefore also varies between realizations. To construct a range-independent WCSSP, a single representative profile from the subset of ITP data was selected and then applied in a range-independent manner over the first 250 km of the propagation track. The Healy data and the interpolation region were handled the same as in the range-dependent case.

In the analysis presented in Sec. 5, the WCSSP realizations are categorized as either

range-dependent or range-independent and as either having a *cooler* (ITP 18, 34, 35) or *warmer* (ITP 69, 78, 86) PSW layer. The number of WCSSP realizations created for use in the acoustic model for each category is listed in Table 1. Because of the inherent spatio-temporal ambiguity present in the ITP measurements, the approach taken here is to examine each set of realizations instead of focusing undue attention on any one realization.

TABLE 1: Number of WCSSP realizations for each category.

	Range-independent	Range-dependent
Cooler PSW	15	14
Warmer PSW	15	17

The acoustic propagation path considered in this work is ice-covered for about 9 months of the year. The scope of the acoustic analysis is restricted to the completely ice-covered scenario; the case of acoustic propagation under partial ice cover is not considered here. An acoustic ray model¹⁶ is used to calculate the acoustic field, where a complex reflection coefficient has been added at the water/ice interface to account for the ice loss as a function of incidence angle. The complex surface reflection coefficient includes the effects of scattering by evaluating the Kirchhoff integral. The Kirchhoff integral was evaluated for intervals of the measured ice draft, using a Gaussian shaded incident beam.^{17,18} The average of 25 evaluations of the Kirchhoff integral calculated for different intervals of the ice draft was used to calculate the surface reflection coefficient used in the propagation model.

The source depth was placed at 150 m, which is nominally in the center of the acoustic duct. A full-field solution was computed in the range/depth plane out to 400 km, which range corresponds to the 150 m bathymetric contour of the continental shelf. The source frequency of the acoustic computation is 250 Hz.

5. Case studies and analysis

Effect of water column variability

To begin this section, Figs. 5(a)–(d) show one realization for each WCCSP category. For example, the upper plot of Fig. 5(a) shows one of fifteen realizations from the range-independent, cooler PSW category. Isospeed contour lines were added to the plot at 1 m/s intervals to help visualize the range variability of the sound speed profile. In Fig. 5(a), the artificially constructed range-independent basin profile is visible out to 250 km. The Healy 2002 data are visible in the shelf region between 310 and 400 km. This portion of the WCSSP is the same for all realizations and all categories. Finally, the interpolation performed in the transition region is visible between 250 and 310 km. The cooler PSW layer is centered around 100 m depth with a sound speed near 1444 m/s. The same speed contour line is visible near 200 m depth. The TL in the range/depth plane, shown in the lower pane of Fig. 5(a), clearly illustrates the presence of an acoustic duct in the basin between these two depths. As the sound reaches the transition region, the duct begins to disappear, and higher transmission loss is encountered as the sound begins to interact with the ice sheet.

Figure 5(b) shows one of fifteen realizations from the range-independent, warmer PSW category. In this case, the depth of the PSW temperature maximum resides near 70 m depth with a maximum sound speed near 1446 m/s. Even though the sound energy is well trapped within the

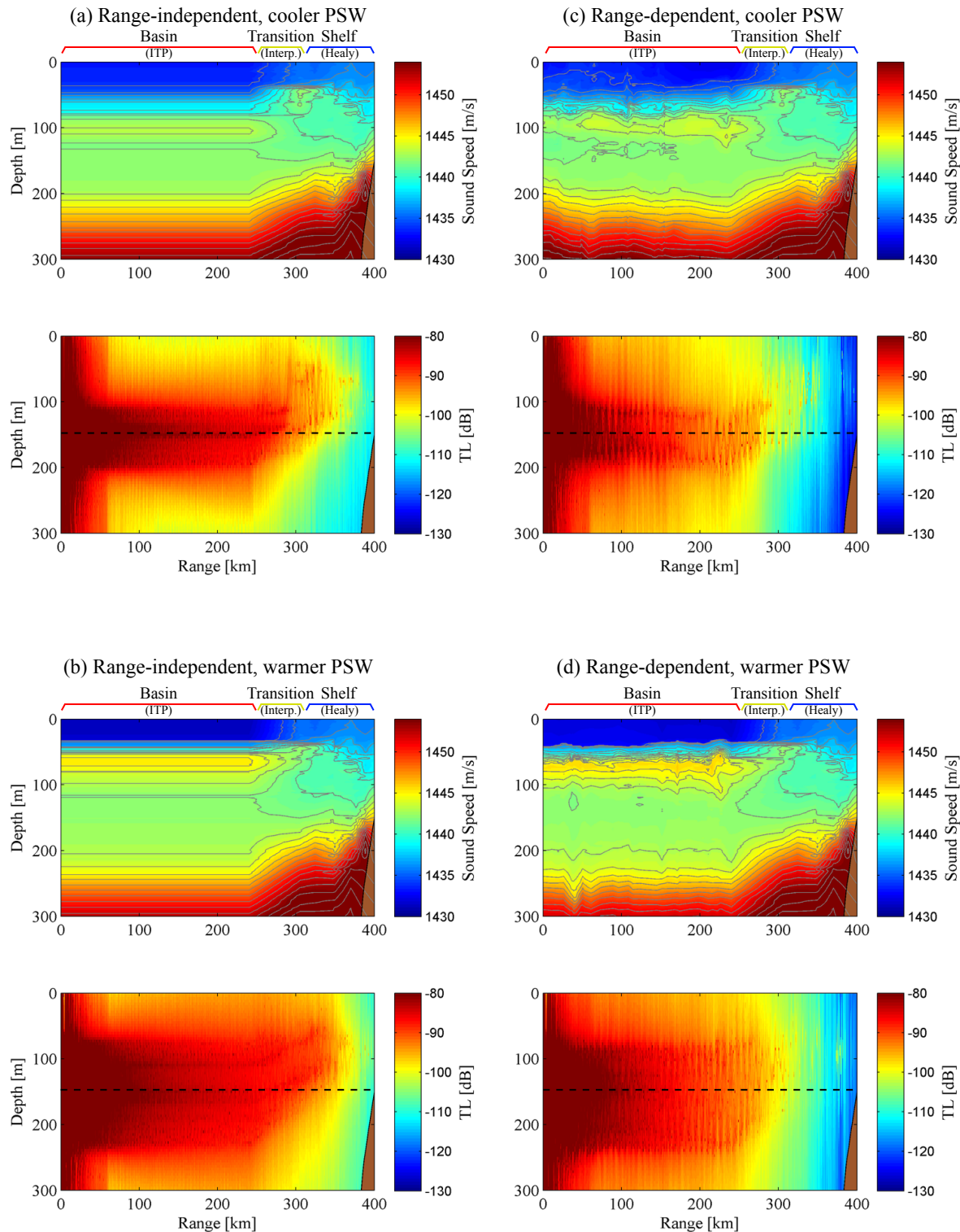


FIGURE 5: WCSSP (upper) and TL (lower) for four representative WCSSP realizations (a)–(d). 1 m/s isospeed contour lines are added to the WCSSP plot to help visualize the range-variability. The source depth of 150 m is indicated on the TL plot by the dashed line.

duct, the TL increases rapidly over the transition and shelf regions as the duct disappears.

Figures 5(c) and (d) each show one realization of a range-dependent cooler and warmer PSW realization. In these cases, the range-variability sampled by the ITP along a cumulative drift distance of 250 km is visible in the first 250 km of each profile. Note that the maximum sound speeds which occur in the PSW layer are similar between the range-independent and range-dependent cases. For both the cooler and warmer PSW realizations shown in the figure, the TL at the 400 km range is larger in the range-dependent cases than it is in the range-independent cases. This suggests that range-variability in the basin-portion of the WCSSP can affect the modeled TL.

For each of the four cases shown in Fig. 5, TL was calculated for multiple realizations of the basin sound speed profile, with the number of realizations in each category described by Table 1. In comparing the calculated acoustic field amongst the types of realizations, TL at a depth of 150 m was considered. This depth is of interest because it is in the acoustic duct, and it is the planned depth of a bottomed moored horizontal line array for the 2016–2017 CANAPE. Transmission loss curves averaged over the number of realizations given in Table 1, are shown by the solid lines in Fig. 6, with shaded areas representing the upper and lower TL bounds from the realizations. Figure 6(a) shows mean TL calculated for range-independent basin profiles [c.f. Figs. 5(a) and (b)]; Fig. 6(b) shows mean TL calculated for range-dependent basin profiles [c.f. Figs. 5(c) and (d)]. In each of the plots, the red line and red shaded area were calculated from basin profiles characterized by a warmer PSW layer; the blue line and blue shaded area were calculated from basin profiles characterized by a cooler PSW layer.

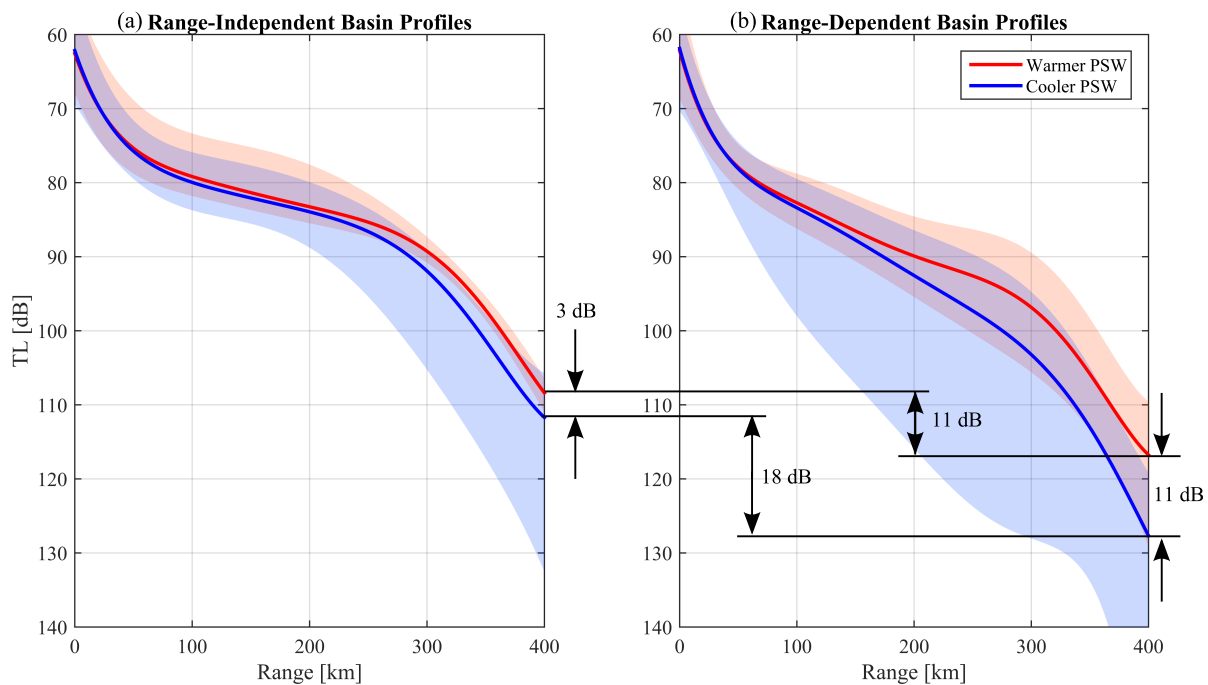


FIGURE 6: Mean TL (solid lines) and range of TL (shaded areas) at 150 m depth for the four types of basin profiles realizations shown in Fig. 5. The means and bounds of TL were calculated from multiple realizations as described by Table 1.

The effect of the temperature of the PSW layer on TL is illustrated in Fig. 6(a) for the range-independent basin profiles. The cooler PSW water produces a weaker sound speed gradient at the upper boundary of the duct, which results in higher loss. At a range of 400 km, the mean profile from the cooler PSW basin profiles is 3 dB lower than that of the warmer PSW basin profiles. A comparison of the bounds of TL, shown by the shaded areas, indicates the cooler PSW results in greater variability with some cases having significantly greater loss than the mean. As the sound speed gradient at the top of the duct weakens, more sound escapes from the duct. In the limiting case for which the sound speed profile is upward refracting, the sound is highly attenuated by the ice cover.

The effect of range-dependence of the basin profiles can be understood by comparing the results in Figs. 6(a) and (b). For the warmer PSW case, the mean TL decreases by 11 dB, and for the cooler PSW case, the mean TL decreases by 18 dB. The bounds of TL are also much greater for the range-dependent basin profiles. For the range-dependent case, the rough boundaries of the duct allow a small amount of sound to continuously scatter out of the duct as it propagates. Another source of variability is cold-core eddies in the PSW layer which locally decrease the sound speed gradient near the top of the duct, resulting in additional sound escaping from the duct. Warm core eddies located in the center of the duct occurred less frequently in the ITP data, but they also caused sound to scatter out of the duct.

Effect of sea ice roughness

The effect of the sea ice roughness was investigated by scaling the measured ice draft. The ice draft measurements were recorded near the North Pole where very rough multi-year ice is expected to be present, flowing in the Transpolar Drift towards Fram Strait. Over the Chukchi Shelf, which is the portion of the propagation path where the WCSSP is upward refracting and where most acoustic interaction with the ice canopy will occur, smoother first-year sea ice is expected to be present.¹⁹ To produce ice draft inputs that might be more consistent with what will be observed on the Chukchi shelf, the measured ice draft data were scaled to reduce the roughness by factors of two and four.

Surface loss calculated using the Kirchhoff integral, evaluated numerically using a Gaussian shaded incident beam^{17,18} for the measured and scaled ice draft are shown by the solid lines in Fig. 7(a). The dip in the curves at 53 degrees is related to the shear speed of the sea ice. The dashed lines were calculated from an empirical model which depends on the standard deviation of the measured ice draft.²⁰ This model is valid for grazing angles less than 20 degrees. The solutions from the Kirchhoff integral and the empirical model are in excellent agreement.

Figure 7(b) shows the mean and bounds of TL at a depth of 150 m calculated for the range-dependent warmer PSW basin profiles and the surface loss curves shown in Figure 7(a). For ranges less than 250 km, the most of the sound is trapped in the sound speed duct, and the effect of surface loss on TL is almost negligible. However, as the sound speed profile transitions to an upward refracting profile on the shelf, the effect of the surface roughness becomes more pronounced. Reducing the surface roughness by a factor of two (four) results in a 9 dB (14 dB) decrease in TL at a range of 400 km.

6. Summary

This manuscript numerically examined environmental parameters affecting acoustic propagation between an acoustic source located in the Canadian Basin and a receiver located on the

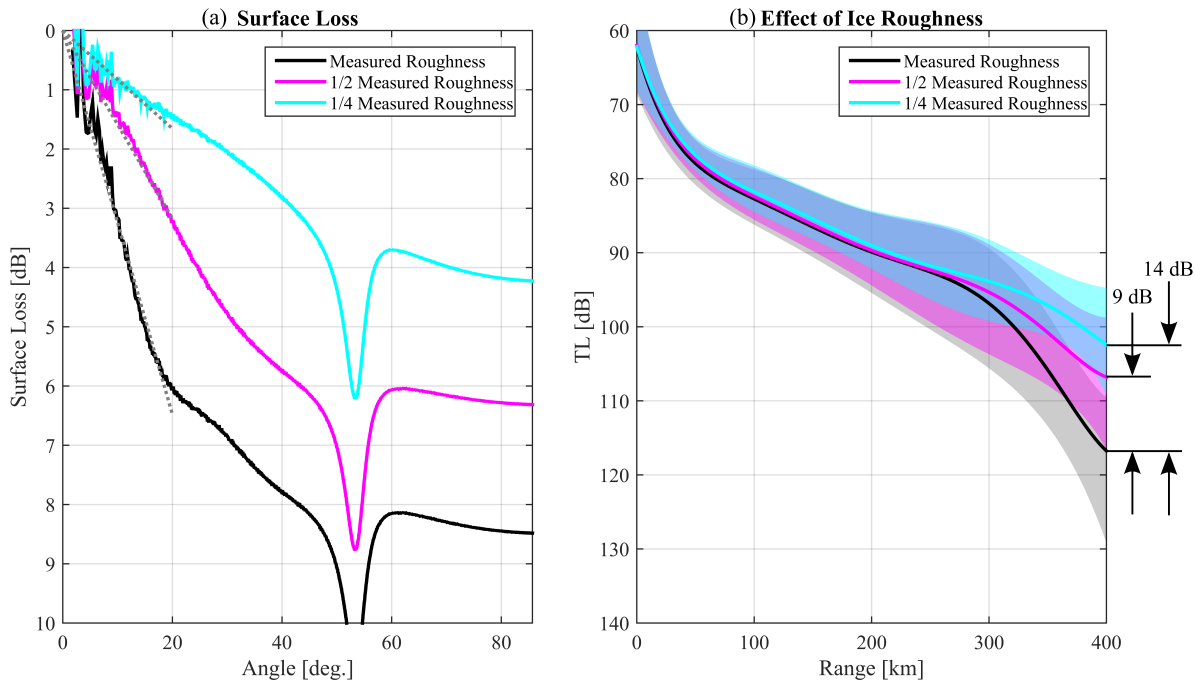


FIGURE 7: (a) Surface loss calculated for varying levels of surface roughness. The solid lines were calculated using the Kirchhoff integral, and gray dotted lines were calculated from the Gordon-Bucker empirical model. (b) Mean TL (solid lines) and range of TL (shaded areas) at 150 m depth for varying levels of ice roughness. The set of warmer PSW range-dependent basin profiles were used in the TL calculations.

Chukchi shelf. The main findings of this study are bounds on the dominant effects on TL over different portions of the acoustic propagation path. A basin profile applied in a range-independent manner bounds the minimum TL and would likely underestimate measured TL by 11 dB to 18 dB. The TL rate within the duct depends on the temperature of the PSW layer forming the upper boundary of the acoustic duct and nominally affects TL by approximately 11 dB at a range of 400 km. Details of the range-dependence of the PSW layer (e.g. eddies) can lead to TL spans between 20 and 40 dB at the receiver for various realizations. Ice scattering loss, which is most important over the shelf, could cause variations in TL of 14 dB at the receiver.

Acknowledgments

This work was sponsored by the Office of Naval Research under Grant Numbers N00014-15-1-2144 and N00014-15-1-2119.

References

- [1] M. Badiey, A. Muenchow, L. Wan, M. S. Ballard, D. P. Knobles, and J. D. Sagers, "Modeling three dimensional environment and broadband acoustic propagation in arctic shelf-basin region," (2014), Vol. 136, pp. 2317–2317.
- [2] E. T. Brugler, R. S. Pickart, G. W. K. Moore, S. Roberts, T. J. Weingartner, and H. Statscewich,

- "Seasonal to interannual variability of the Pacific water boundary current in the Beaufort Sea," *Progress in Oceanography* **127**, 1–20 (2014).
- [3] M. Steele, J. Morison, W. Ermold, I. Rigor, M. Ortmeyer, and K. Shimada, "Circulation of summer Pacific halocline water in the Arctic Ocean," *Journal of Geophysical Research: Oceans* **109** (2004). C02027.
 - [4] R. S. Pickart, T. J. Weingartner, L. J. Pratt, S. Zimmermann, and D. J. Torres, "Flow of winter-transformed pacific water into the western arctic," *Deep Sea Research Part II: Topical Studies in Oceanography* **52**, 3175 – 3198 (2005). The Western Arctic Shelf-Basin Interactions (SBI) Project.
 - [5] M. A. Spall, R. S. Pickart, P. S. Fratantoni, and A. J. Plueddemann, "Western Arctic shelfbreak eddies: formation and transport," *Journal of Physical Oceanography* **38**, 1644–1668 (2008).
 - [6] The Ice-Tethered Profiler data were collected and made available by the Ice-Tethered Profiler Program (Toole et al., 2011; Krishfield et al., 2008) based at the Woods Hole Oceanographic Institution (<http://www.whoi.edu/itp>).
 - [7] J. T. Mathis, R. S. Pickart, D. A. Hansell, D. Kadko, and N. R. Bates, "Eddy transport of organic carbon and nutrients from the Chukchi Shelf: Impact on the upper halocline of the western Arctic Ocean," *Journal of Geophysical Research: Oceans* **112** (2007). C05011.
 - [8] R. D. Meunch, J. T. Gunn, T. E. Whitledge, P. Schlosser, and W. J. Smethie, "An Arctic Ocean cold core eddy," *Journal of Geophysical Research* **105**, 23997–24006 (2000).
 - [9] M. L. Timmermans, J. Toole, A. Proshutinsky, R. Krishfield, and A. Plueddemann, "Eddies in the Canada Basin, Arctic Ocean, observed from ice-tethered profilers," *Journal of Physical Oceanography* **38**, 133–145 (2008).
 - [10] M. Zhao, M.-L. Timmermans, S. Cole, R. Krishfield, A. Proshutinsky, and J. Toole, "Characterizing the eddy field in the Arctic Ocean halocline," *Journal of Geophysical Research: Oceans* **119**, 8800–8817 (2014).
 - [11] J. M. Toole, M.-L. Timmermans, D. K. Perovich, R. A. Krishfield, A. Proshutinsky, and J. A. Richter-Menge, "Influences of the ocean surface mixed layer and thermohaline stratification on Arctic Sea ice in the central Canada Basin," *Journal of Geophysical Research: Oceans* **115**, C10018 (2010).
 - [12] The data were collected and made available by the Shelf-Basin Interaction project at WHOI (aon.whoi.edu).
 - [13] The data were collected and made available by the Beaufort Gyre Exploration Program based at the Woods Hole Oceanographic Institution (<http://www.whoi.edu/beaufortgyre>) in collaboration with researchers from Fisheries and Oceans Canada at the Institute of Ocean Sciences.
 - [14] National Snow and Ice Data Center (NSIDC), "Submarine upward looking sonar ice draft profile data and statistics, version 1." URL <http://dx.doi.org/10.7265/N54Q7RWK>.
 - [15] M. Jakobsson, L. Mayer, B. Coakley, J. A. Dowdeswell, S. Forbes, B. Fridman, H. Hodnesdal, R. Noormets, R. Pedersen, M. Rebesco, H. W. Schenke, Y. Zarayskaya, D. Accettella,

- A. Armstrong, R. M. Anderson, P. Bienhoff, A. Camerlenghi, I. Church, M. Edwards, J. V. Gardner, J. K. Hall, B. Hell, O. Hestvik, Y. Kristoffersen, C. Marcussen, R. Mohammad, D. Mosher, S. V. Nghiem, M. T. Pedrosa, P. G. Travaglini, and P. Weatherall, “The international bathymetric chart of the arctic ocean (ibcao) version 3.0,” *Geophysical Research Letters* **39** (2012).
- [16] M. B. Porter and H. P. Bucker, “Gaussian beam tracing for computing ocean acoustic fields,” *The Journal of the Acoustical Society of America* **82**, 1349–1359 (1987).
- [17] E. I. Thorsos, “The validity of the Kirchhoff approximation for rough surface scattering using a Gaussian roughness spectrum,” *The Journal of the Acoustical Society of America* **83**, 78–92 (1988).
- [18] M. J. Isakson, N. P. Chotiros, R. Abraham Yarbrough, and J. N. Piper, “Quantifying the effects of roughness scattering on reflection loss measurements,” *The Journal of the Acoustical Society of America* **132**, 3687–3697 (2012).
- [19] M. Shokr and N. K. Sinha, eds., *Sea Ice: Physics and Remote Sensing*, 68–76 (Wiley, 2015).
- [20] D. F. Gordon and H. P. Bucker, “Arctic acoustic propagation model with ice scattering,” Tech. Rep. 985, Naval Ocean Systems Center, San Diego CA 92152 (1984).